Raport Badawczy
Research Report

RB/7/2014

A wavelet model for wind velocity and gusts of wind

J. Jarnicka

Instytut Badań Systemowych
Polska Akademia Nauk

Systems Research Institute
Polish Academy of Sciences

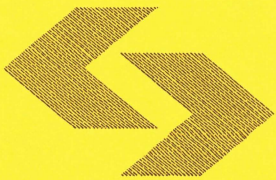

POLSKA AKADEMIA NAUK

Instytut Badań Systemowych

ul. Newelska 6

01-447 Warszawa

tel.: (+48) (22) 3810100

fax: (+48) (22) 3810105

Kierownik Zakładu zgłaszający pracę:
Prof. dr hab. inż. Zbigniew Nahorski

Warszawa 2014

A WAVELET MODEL FOR WIND VELOCITY AND GUSTS OF WIND

JOLANTA JARNICKA
SYSTEMS RESEARCH INSTITUTE
POLISH ACADEMY OF SCIENCES
NEWELSKA 6, 01-447 WARSAW, POLAND
EMAIL: JOLANTA.JARNICKA@IBSPAN.WAW.PL

ABSTRACT. The wavelet transform is one of the well-known tools, used for signal processing and modelling, and being applied to various types of data. In this paper, a wavelet model is introduced to describe the wind velocity and gusts of wind. The analysis is concentrated on the discrete wavelet transform, based on the Haar and Daubechies wavelets. The goal is to approximate the data by wavelets as well as to 'denoise' them by thresholding.

1. INTRODUCTION

Wavelet transform is one of the well-known and widely used tools for signal analysis. Particularly noteworthy is the discrete wavelet transform, – a computationary efficient technique to analyze non-stationary data. One of the reasons wavelets have been successful in many fields, such as image compression is their ability to efficiently represent all manner of complicated signals. Wavelets are particularly effective at representing signals with discontinuities, due to their excellent localization properties. In this paper we conduct a multiresolution analysis of the data on wind velocity and gusts of wind, using wavelet representation. The idea of using wavelets to describe physical phenomena, like wind is nothing new. The methods of wavelet transform have already been used e.g. in [1], [2].

In general, wavelets are functions satisfying certain requirements. The name comes from the fact that, they should integrate to zero, waving above and below the x-axis. There are many kinds of wavelets – smooth, compactly supported, given by simple mathematical expressions, having simple associated filters, etc. The details on the wavelets theory can be found e.g in [6], [3], we will only shorty recall some facts, concerning the wavelet transform, in particular the discrete wavelet transform.

Consider a function $\psi(\cdot) \in \mathcal{L}^2(\mathbb{R})$, such that $\int_{\mathbb{R}} \psi(x)\,dx = 0$ and let dilations and translations of the function $\psi(\cdot)$ be given by

$$\psi_{j,k}(x) = 2^{-\frac{j}{2}}\psi(2^{-j}x - k), \quad \text{for} \quad j,k \in \mathbb{Z}, \quad \text{where } x \in \mathbb{R}. \tag{1}$$

The function $\psi(\cdot)$ is called a *wavelet* (or a *mother wavelet*), when the family $\{\psi_{j,k}(\cdot)\}_{j,k\in\mathbb{Z}}$ forms an orthonormal basis on $\mathcal{L}^2(\mathbb{R})$, the vector space of measurable, square integrable functions of a single variable. The dilation parameter j controls the scale (or size) of the wavelet and the translation parameter k controls the location of the wavelet. It is easy to observe that, scale factor $2^{\frac{j}{2}}$ normalizes the wavelet basis element $\psi_{j,k}$, for $j,k \in \mathbb{Z}$, so that $||\psi_{j,k}|| = ||\psi||$, where the norm $||\cdot||$ is generated by the inner product $<\cdot,\cdot>$. In the wavelet transform, given a function f, we want to approximate that function in terms of the wavelet basis (1), i.e.

$$f(x) = \sum_j \sum_k d_{j,k}\psi_{j,k}(x), \quad j,k \in \mathbb{Z}, \tag{2}$$

where $d_{j,k}$, $j,k \in \mathbb{Z}$ are the *wavelet coefficients*.

A simple example of a wavelet basis is the Haar basis, generated from the mother wavelet (called the *Haar wavelet*)

$$\psi(x) = \begin{cases} 1, \text{if } x \in [0, \frac{1}{2}), \\ -1, \text{if } x \in [\frac{1}{2}, 1), \\ 0, \text{otherwise}, \end{cases} \tag{3}$$

illustrated in Fig.1.1. It is easy to check that the wavelets derived from the mother Haar wavelet form an orthonormal basis, by observing that (see [5]):

- wavelets with different translate numbers k, but on the same scale j do not have intersecting supports,
- wavelets on different scales j either have non-intersecting supports or, one wavelet takes the value $-C$ and then C over a set where the other wavelet is constant (for some C),
- $< \psi_{j,k}, \psi_{j,k} >= 1$, for all j, k.

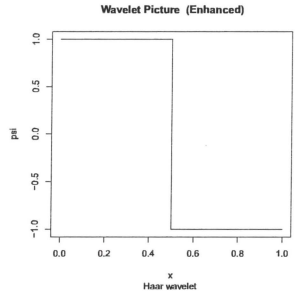

Fig.1.1 Haar wavelet $\psi(x)$, given by (3).

There are also many other families of wavelets, arising form mother wavelets more regular than the Haar function (3). One should mention two families of Daubechies wavelets (see [5] or [4]), namely the *extremal phase* or *least-asymmetric* wavelets. The wavelets in each of these have compact support. Moreover, indexing each mother wavelet in a family by N, the regularity of the mother wavelet (and hence all the derived wavelets) is proportional to N, i.e. if N increases, they become smoother.

1.1. **Data on wind velocity and gusts of wind.** The data set to be analyzed provides the information on various properties of wind, such as the measurements of wind velocity, direction, gusts of wind etc., collected between the 1st and the 4th Jan, 2011. The measurements were performed every 9 minutes, starting at midnight 1st of Jan, and ending with 23.40, 4th of January, 2011. The goal of the paper is to find a wavelet model for two data sets – on wind velocity and gusts of wind.

1.2. **Haar wavelets on functions.** Given two data sets that, need to be analyzed, we are interested in wavelet representations of functions generated by (finite) data sets, in particular on $[0, 1]$.

Let $\mathbf{y} = (y_1, y_2, \ldots, y_n)$ be a data vector, such that $y_i \in \mathbb{R}$, for $i = 1, \ldots, n$. Assume that $n = 2^J$, where $J > 0$. The sequence satisfying that condition is called a *dyadic* one. Each data vector $\mathbf{y}$ of size 2^J, where $J > 0$, can be associated with a piecewise constant function f given on $[0, 1]$, generated as follows (see [4])

$$f(x) = \sum_{k=0}^{2^J-1} y_{k+1} \cdot \mathbf{1}(k2^{-J} \leq x < (k+1)2^{-J}),$$

where $\mathbf{1}$ denotes an indicator of the given set.

This data function is in the $\mathcal{L}^2([0,1])$ space. To illustrate that, consider the data on wind velocity. Since $n = 546$, the data vector is truncated to a dyadic-length sequence, of $n = 512 = 2^9$. Figure 1.2 below shows the data (a) in the original form (for $n = 512$) and (b) in the form of the data function.

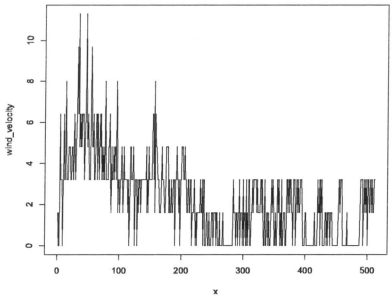

Fig.1.2 (a). Data on wind velocity, original sequence

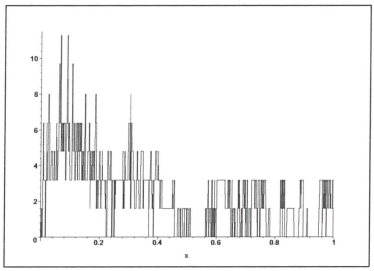

Fig.1.2 (b) data function on $[0,1]$.

Multiresolution analysis provides the framework for examining functions at different scales. The information we extract from the vector $(y_1, y_2, \ldots, y_{2^J})$ in "detail" is given by *wavelet coefficients* $d_{j,k}$, and the information concerning a scale is given by *scaling coefficients* $c_{j,k}$, also known as *father wavelets coefficients*. The coefficients are obtained by a pyramid algorithm (see e.g.[4], [3]). We have

$$dk = \alpha(y_{2k} - y_{2k-1}), \quad ck = \alpha(y_{2k} + y_{2k+1}),$$

where $\alpha = 2^{-\frac{1}{2}}$. More general form of d_k and c_k is given by

$$d_k = \sum_{l \in \mathbb{Z}} g_l y_{2k-1},$$

$$ck = \sum_{l \in \mathbb{Z}} h_l y_{2k-l},$$

where the filtering functions are of the form

$$g_l = \begin{cases} 2^{-\frac{1}{2}}, \text{for } l = 0, \\ -2^{-\frac{1}{2}}, \text{for } l = 1, \\ 0, \text{otherwise}, \end{cases} \qquad h_l = \begin{cases} 2^{-\frac{1}{2}}, \text{for } l = 0, \\ -2^{-\frac{1}{2}}, \text{for } l = 1, \\ 0, \text{otherwise}. \end{cases}$$

Each of the above sequences can be obtained at a given resolution $j = J-1$, where $n = 2^J$, which gives $\{d_{j,k}\}$, and $\{c_{j,k}\}$, $j = 0, \ldots, J-1$ and $k = 0, \ldots, 2^j - 1$.

1.3. **Scaling coefficients (father wavelets coefficients).** . The coefficients $\{c_{J,k}\}$, where $J > 0$ and $k = 0, \ldots, 2^J - 1$ can also be considered in a different way (see [4]). Define the *Haar father wavelet*

$$\phi(x) = \begin{cases} 1, \text{if } x \in [0,1), \\ 0, \text{otherwise.} \end{cases} \tag{4}$$

Dilations and translations of the function (4) become

$$\phi_{J,k}(x) = 2^{\frac{J}{2}}\phi(2^J x - k) = \begin{cases} 2^{\frac{J}{2}}, \text{if } x \in [2^{-J}k, 2^{-J}(k+1)], \\ 0, \text{ otherwise.} \end{cases}$$

Let now the finest-level (scale 2^J) father wavelets coefficients be of the form

$$c_{J,k} = \int_0^1 f(x)\phi_{J,k}(x)\,dx =< f, \phi_{J,k} >, \tag{5}$$

where $< \cdot, \cdot >$ denotes an inner product on $\mathcal{L}^2[0,1]$.

The coefficient (5) is just an integral of $f(x)$ (given on $[0,1]$) on the interval $I_{J,k} = [2^{-J}k, 2^{-J}(k+1)]$, and proportional to the local average of $f(x)$ over the interval $I_{J,k}$. In fact, the scaling coefficients $\{c_{J,k}\}_{k=0}^{2^J-1}$, given by (5) and the associated Haar father wavelets (4) define an approximation of $f(x)$, given by

$$f_J(x) = \sum_{k=0}^{2^J-1} c_{J,k}\phi_{J,k}(x).$$

Additionally, the father wavelet approximation f_{j+1} at finer scale $j+1$, where $j = 0, \ldots, J-1$, can be obtained by the following rule

$$\begin{aligned} f_1(x) &= c_{0,0}\phi(x) + d_{0,0}\psi(x), \\ f_{j+1}(x) &= f_j(x) + \sum_{k=0}^{2^J-1} d_{j,k}\psi_{j,k}(x), \end{aligned} \tag{6}$$

where

$$f_j(x) = \sum_{k=0}^{2^j-1} c_{j,k}\phi_{j,k}(x), \tag{7}$$

what gives the *wavelet model of the function* $f(x)$ on $[0,1]$

$$f(x) = c_{0,0}\phi(x) + \sum_{j=0}^{J-1}\sum_{k=0}^{2^j-1} d_{j,k}\psi_{j,k}(x), \tag{8}$$

where $\psi_{j,k}(x) = 2^{-\frac{j}{2}}\psi(2^{-j}x - k)$.

Note also that, since the set $\{\psi_{j,k}(x)\}_{j,k\in\mathbb{Z}}$ forms an orthonormal basis on $\mathcal{L}^2$, functions $\{\phi_{j,k}(x)\}_{k\in\mathbb{Z}}$ for each $j \in \mathbb{Z}$ are orthonormal bases for spaces V_j, $j \in \mathbb{Z}$, such that

$$\ldots V_{-1} \subset V_0 \subset V_1 \subset \ldots$$

In such a case, functions

$$f_j(x) = \sum_{k\in\mathbb{Z}} c_{j,k}\phi_{j,k}(x) = P_j f, \quad \text{where} \quad j \in \mathbb{Z},$$

can be treated as projections of f onto the space V_j.

2. Case study 1. Modelling wind velocity

Given the sequence $(y_1, y_2, \ldots, y_n)$, where $n = 2^J$, the *discrete wavelet transform* can be performed, due to (6)-(7), using the Haar wavelets.
The wavelet decomposition has the following form

$$f(x) = c_{0,0}\phi(x) + \sum_{j=0}^{J-1} \sum_{k=0}^{2^j-1} d_{j,k}\psi_{j,k}(x),$$

where $\psi_{j,k}(x) = 2^{-\frac{j}{2}}\psi(2^{-j}x - k)$.

This means that a vector of wavelet coefficients $\{d_{j,k}\}$ for $j = 0, \ldots, J-1$ and $k = 0, \ldots, 2^j - 1$ is produced, together with the last father wavelet coefficient $c_{0,0}$. We are also interested in the scaling coefficients $c_{j,k}$ (aka father wavelet coefficients).

The analysis is carried out by the use of the `threshold` package in R. The goal is to approximate the data vector by wavelets, as well as to denoise them by thresholding.

The data on wind velocity are depicted in Figure 2.1.

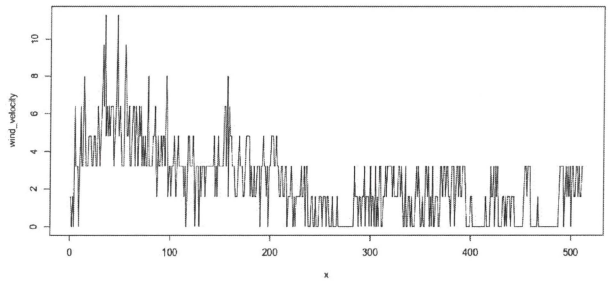

Fig. 2.1 Wind velocity data.

To find the coefficients in the model (8), we use R and the `WaveThresh` package with `wd` function. Since $n = 512 = 2^9$, we get $J = 9$, and hence $j = 0, \ldots, 8$. The wavelets coefficients $\{d_{j,k}\}$ obtained are presented below, for levels $j = 0, \ldots, 8$.

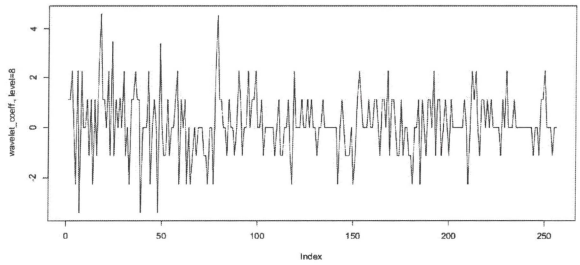

Fig. 2.2. Highest resolution ($j = 8$) wavelet coefficients $d_{8,k}$, $k = 0, \ldots, 2^8 - 1$, Haar wavelets, data on wind velocity.

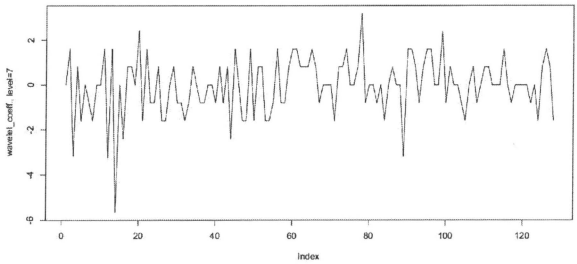

Fig. 2.3. Wavelet coefficients $d_{7,k}$, on the level of $j = 7$, $k = 0, \ldots, 2^7 - 1$ Haar wavelets, data on wind velocity.

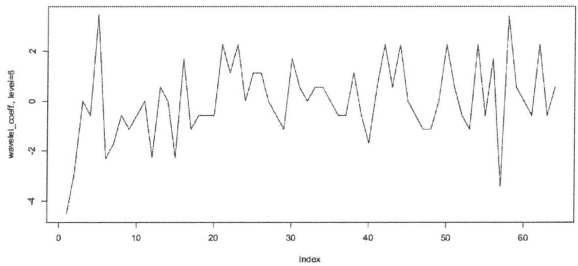

Fig. 2.4. Wavelet coefficients $d_{6,k}$, on the level of $j = 6$, $k = 0, \ldots, 63$ Haar wavelets, data on wind velocity.

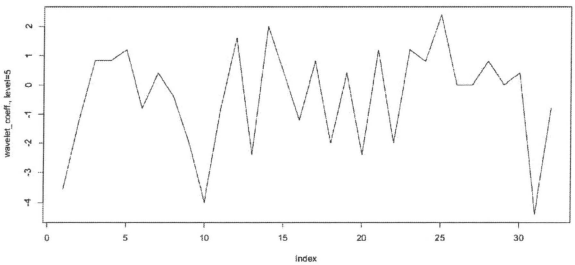

Fig. 2.5. Wavelet coefficients $d_{5,k}$, on the level of $j = 5$, $k = 0, \ldots, 31$ Haar wavelets, data on wind velocity.

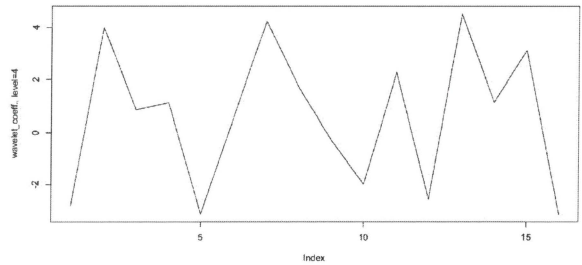

Fig. 2.6. Wavelet coefficients $d_{4,k}$, on the level of $j = 4$, $k = 0, \ldots, 15$ Haar wavelets, data on wind velocity.

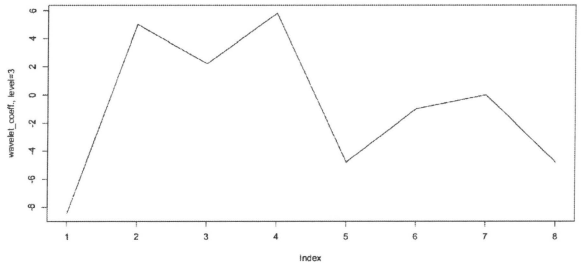

Fig. 2.7. Wavelet coefficients $d_{3,k}$, on the level of $j = 3$, $k = 0, \ldots, 7$ Haar wavelets, data on wind velocity.

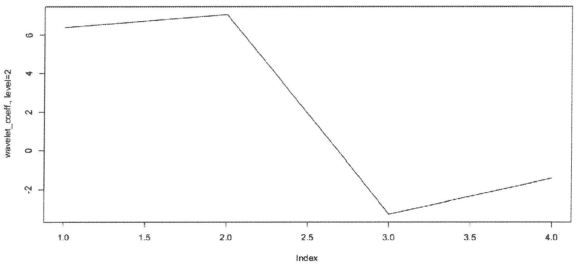

Fig. 2.8. Wavelet coefficients $d_{2,k}$, on the level of $j = 2$, $k = 0, \ldots, 3$ Haar wavelets, data on wind velocity.

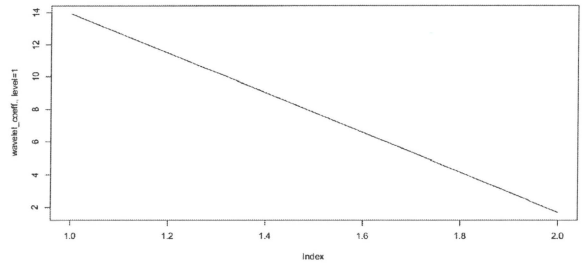

Fig. 2.9. Wavelet coefficients $d_{1,k}$, on the level of $j = 1$, $k = 0, \ldots, 1$ Haar wavelets, data on wind velocity.

The last wavelet coefficient $d_{0,0} = 24.766$, and $c_{0,0} = 52.626$.

Having obtained the results, we can see that, some wavelets coefficients for high level resolution $j = 8$ and $j = 7$ are equal zero, and for some we can observe getting the same values. This is a good illustration of a sparsity of a wavelet representation (it can also be seen in Fig. 2.2), as only few of coefficients are non-zero. One can also observe that the coefficients get progressively bigger (in absolute size), when the level decreases.

The results obtained are also presented in Figure 2.10.

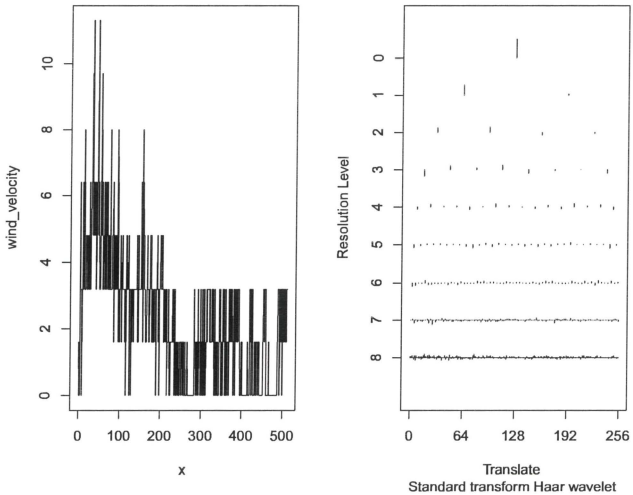

Fig.2.10 Haar discrete wavelet coefficients $d_{j,k}$, $j = 0, \ldots, J-1$, $k = 0, \ldots, 2^j - 1$, data on the wind velocity.

To get the scaling coefficients (father wavelet coefficients), for scales $j = 1, \ldots, 8$, we use `R` and packages `Wavethresh` and `wavelets`. The results obtained can be seen in Figure 2.11.

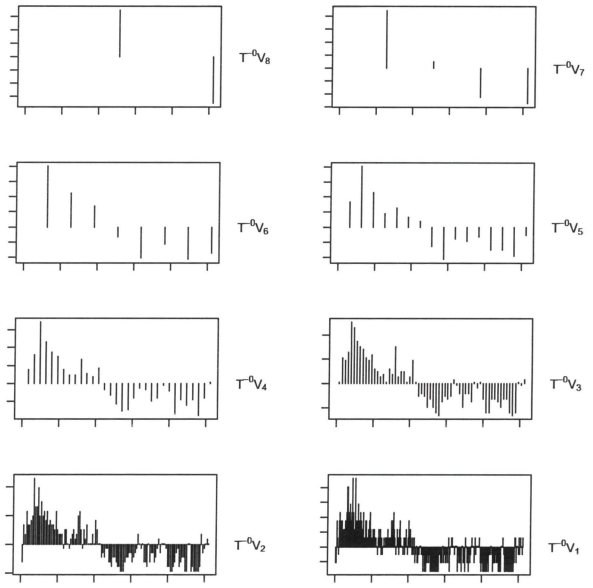

Fig. 2.11 Scaling coefficients $c_{j,k}$, for $j = 1, \ldots, 8$ as approximations to the data on wind velocity (where $n = 2^9$), $c_{0,0} = 52.62642$.

Using the results obtained we can exactly reconstruct the original data on wind velocity. We will do this and compare it to the original. The inverse discrete wavelet transform is conducted using the function `wr`, which stands for wavelet reconstruction. Reconstructing the data, we get

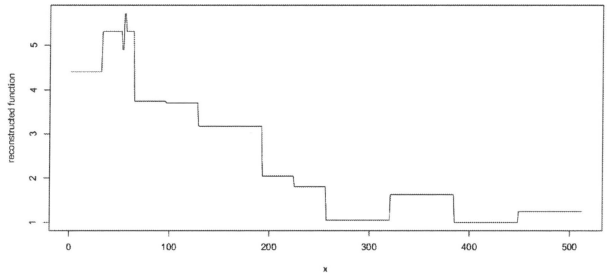

Fig. 2.12. Wavelet reconstruction of the original data on wind velocity, Haar wavelets.

To check that the reconstruction is exactly the same, up to numerical error, we can subtract the original data from the reconstruction and look at the error. It is small, it equals 9.769963e-15.

To the end of that section, we apply the thresholding to the coefficients obtained above, using the universal policy and the function `threshold`. The results are depicted in Figure 2.13 b).

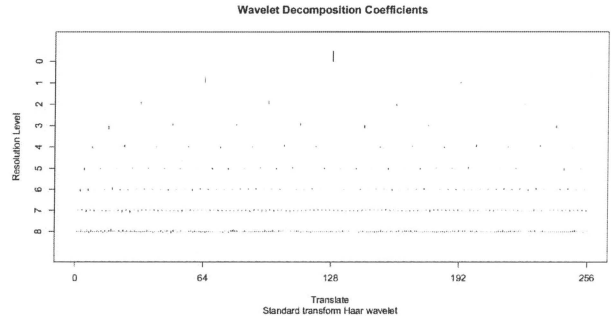

Fig. 2.13.a) Wavelet coefficients, standard Haar transform.

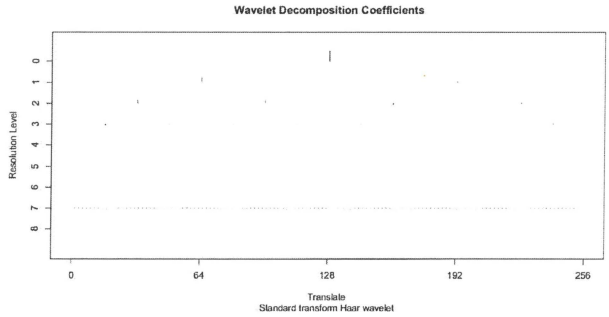

Fig. 2.13.b) Wavelet coefficients after universal thresholding.

It can be observed that some of the smaller coefficients have disappeared after thresholding, when compared with Figure 2.13 a). The reconstructed data, after thresholding are presented in Figure 2.14.

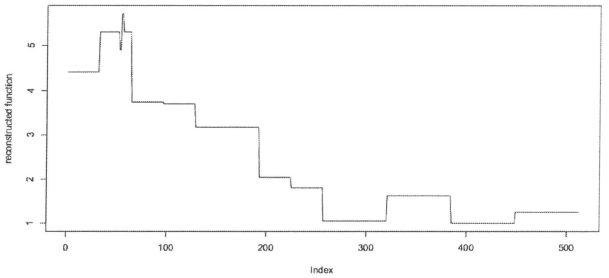

Fig. 2.14. Wavelet reconstruction of the data on wind velocity after universal thresholding Haar wavelets.

3. Case study 2. Modelling gusts of wind

Now we consider the data on gusts of wind. As previously, the data vector is of the length $n = 546$, and need to be truncated to a dyadic one. We get

$$\mathbf{y} = (y_1, y_2, \ldots, y_n),$$

where $n = 512 = 2^9$, $J = 9$. Therefore $j = 0, \ldots, 8$, and $k = 0, \ldots, 2^j - 1$. The data vector $\mathbf{y}$ is depicted in Figure 3.1

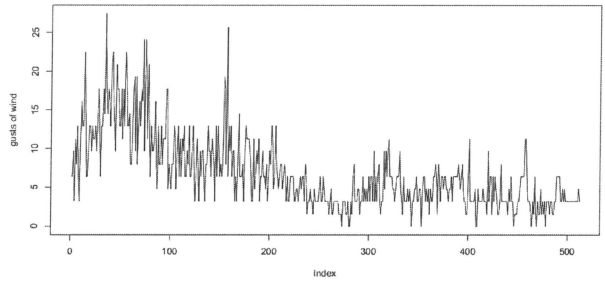

Fig. 3.1 Data on gusts of wind.

As previously, we are interested in the discrete wavelet transform (using the Haar basis), i.e.in the wavelet coefficients in the model (8), given by The wavelet decomposition has the following form

$$f(x) = c_{0,0}\phi(x) + \sum_{j=0}^{J-1} \sum_{k=0}^{2^j-1} d_{j,k}\psi_{j,k}(x),$$

where $\psi_{j,k}(x) = 2^{-\frac{j}{2}}\psi(2^{-j}x - k)$. To perform the analysis, we use R, and its `WaveThresh` package. The results obtained can be seen in Figure 3.2.

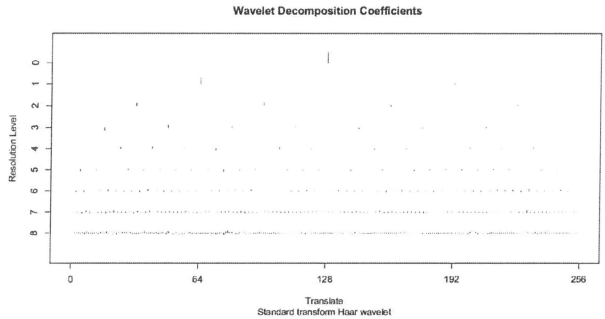

Fig. 3.2 Wavelet coefficients $d_{j,k}$, Haar wavelets data on gusts of wind.

Figure 3.3 presents the father wavelet coefficients obtained for all levels of resolution: $j = 1, \ldots, 8$.

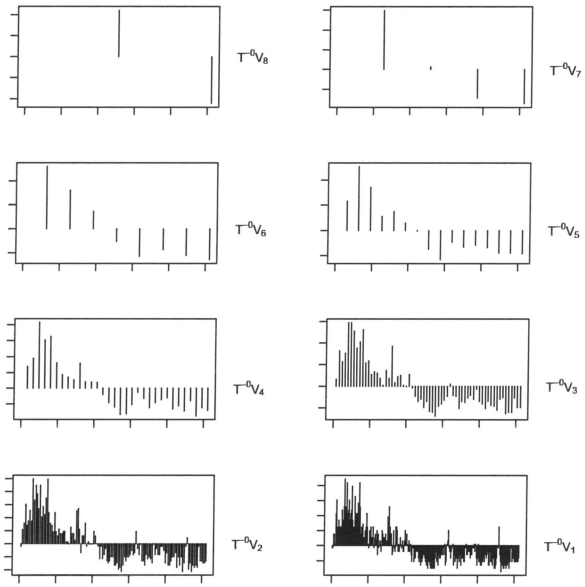

Fig. 3.3 Scaling coefficients as approximations to the data on gusts of wind, levels $j = 1, \ldots, 8$

The last father wavelet coefficient is equal $c_{0,0} = 155.8154$.

Reconstructing the data on gusts of wind from the wavelet coefficients, we get the results (Figure 3.4) really close to the original data, presented in Figure 3.1. The absolute error, obtained by subtracting the original data on gusts of wind from the reconstructed ones is small, equals 2.842171e-14.

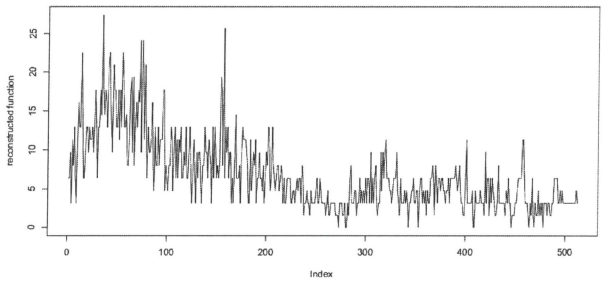

Fig. 3.4. Wavelet reconstruction of the data on gusts of wind, Haar wavelets.

As in Section 2, we are also interested in thresholding, using universal policy. The coefficients obtained after thresholding and the reconstructed data on gusts of wind are given in Figures 3.5 and 3.6, respectively.

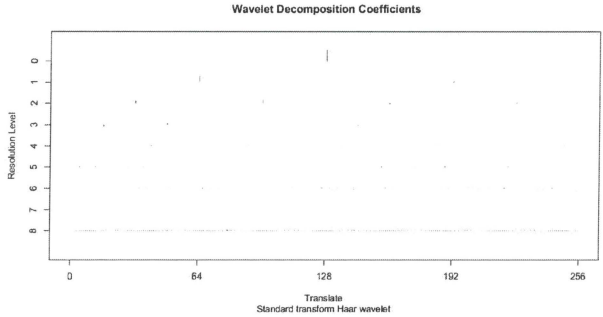

Fig. 3.5. Wavelet coefficients after universal thresholding, Haar wavelets, data on gusts of wind.

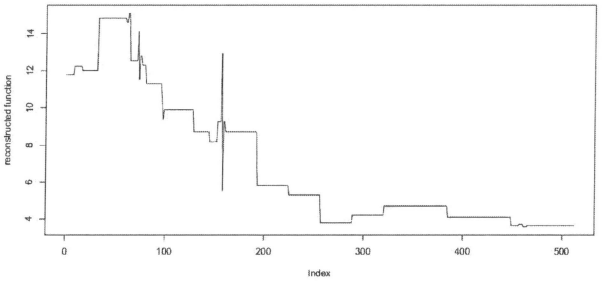

Fig. 3.6. Reconstruction of the data on gusts of wind after universal thresholding, Haar wavelets.

4. Daubechies wavelets

The analysis conducted in Sections 2 and 3, was based on the Haar wavelets, generated from the mother wavelet (3). It is the first wavelet in the more regular and compactly supported `DaubExPhase` family of Daubechies wavelets (see e.g.[5], [4], [3],etc.). It consists of 10 members, having filters from 1 to 10.

For comparison, therefore, we present here the discrete wavelet transform based on the Daubechies wavelets from this family, with filter $N = 2$ and $N = 10$.

We are interested in both data sets under consideration – data on wind velocity (analyzed in Section 2) and data on gusts of wind (analyzed in Section 3). The results are presented below.

4.1. **Data on wind velocity.**

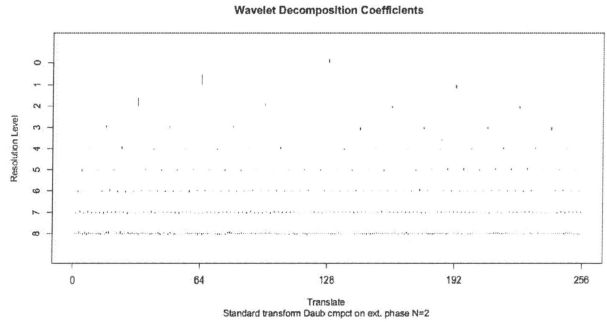

Fig. 4.1. Wavelet coefficients, `DaubExPhase`, with filter $N = 2$, data on wind velocity.

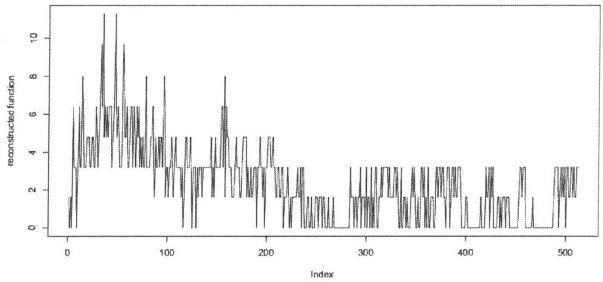

Fig. 4.2. Wavelet reconstruction of the data on wind velocity, `DaubExPhase`, with filter $N = 2$.

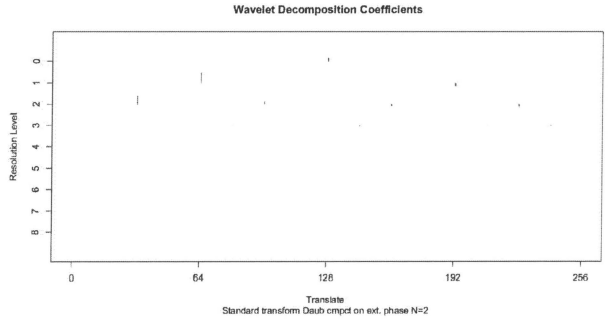

Fig. 4.3. Wavelet coefficients after universal thresholding, `DaubExPhase`, with filter $N = 2$, data on wind velocity.

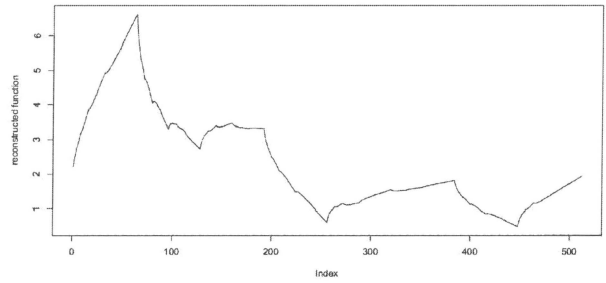

Fig. 4.4. Reconstruction of the data on wind velocity after universal thresholding, `DaubExPhase`, with filter $N = 2$.

The results presented in Figures 4.1-4.4 are slightly better than the ones obtained in Section 2. In particular, the reconstruction of the data, depicted in Figure 4.2 describes the original data in a more accurate way (when compared with Figure 2.12). The absolute error is equal 5.840306e-11. Applying the `DaubExPhase` wavelets with filter $N = 10$, gives even better results.

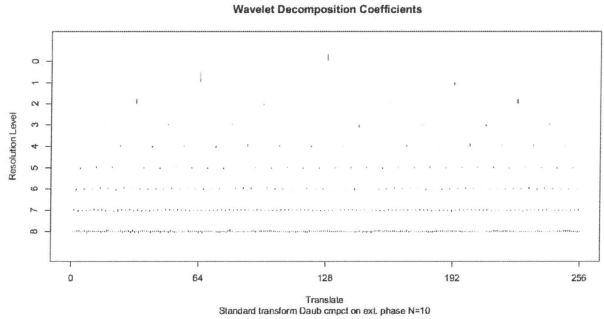

Fig. 4.5. Wavelet coefficients, `DaubExPhase`, with filter $N = 10$, data on wind velocity.

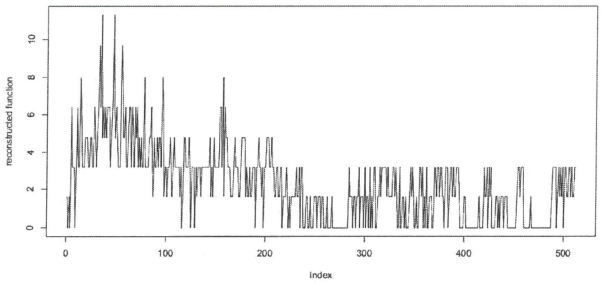

Fig. 4.6. Wavelet reconstruction of the data on wind velocity, `DaubExPhase`, with filter $N = 10$.

The absolute error is small, it equals 1.583791e-10, and the reconstruction after universal thresholding becomes smooth (Figure 4.8).

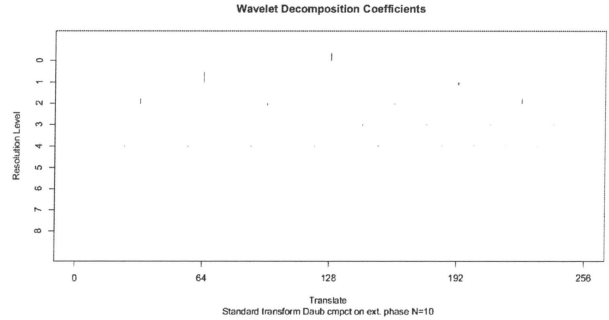

Fig. 4.7. Wavelet coefficients after universal thresholding, `DaubExPhase`, with filter $N = 10$, data on wind velocity.

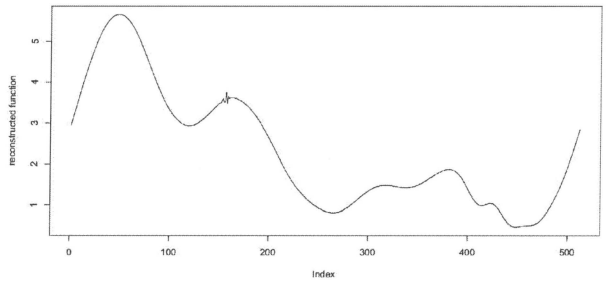

Fig. 4.8. Reconstruction of the data on wind velocity after universal thresholding, `DaubExPhase`, with filter $N = 10$.

4.2. Data on gusts of wind.

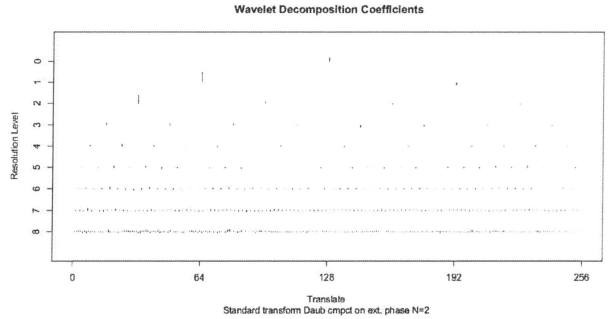

Fig. 4.9. Wavelet coefficients, `DaubExPhase`, with filter $N = 2$, data on gusts of wind.

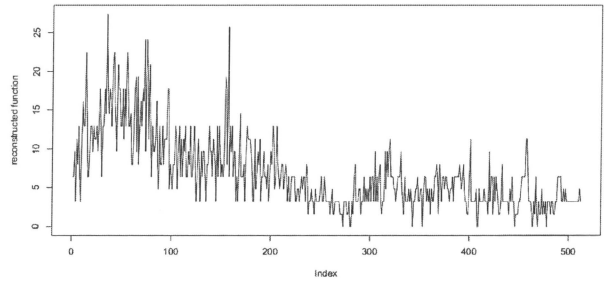

Fig. 4.10. Wavelet reconstruction of the data on gusts of wind, `DaubExPhase`, with filter $N = 2$.

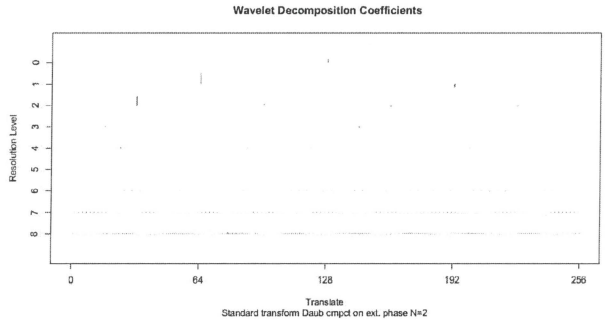

Fig. 4.11. Wavelet coefficients after universal thresholding, `DaubExPhase`, with filter $N = 2$, data on gusts of wind.

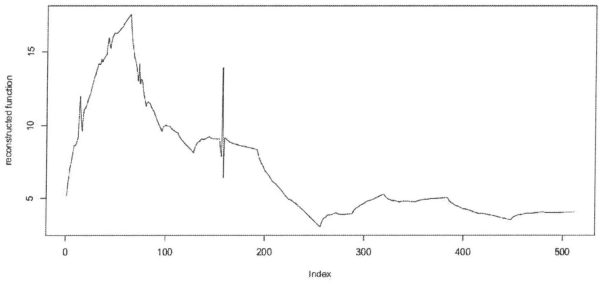

Fig. 4.12. Reconstruction of the data on gusts of wind after universal thresholding, `DaubExPhase`, with filter $N = 2$.

The results presented in Figures 4.9-4.12 are better than the ones obtained in Section 3. We can seen that, the reconstructed data are almost the same as the original ones, the absolute

error,obtained by subtracting the data on gusts of wind form the reconstructed ones, is equal 1.548557e-10. Applying the `DaubExPhase` wavelets with filter $N = 10$, gives even better results.

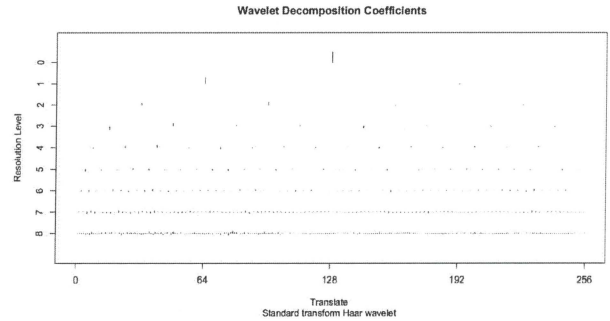

Fig. 4.13. Wavelet coefficients, `DaubExPhase`, with filter $N = 10$, data on gusts of wind.

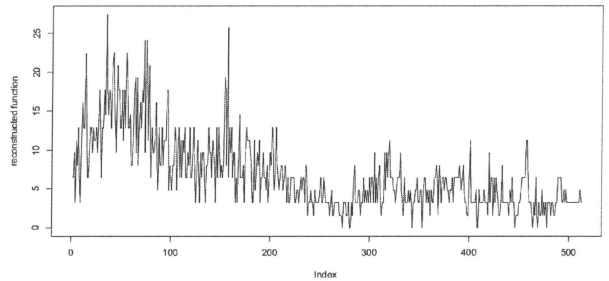

Fig. 4.14. Wavelet reconstruction of the data on gusts of wind, `DaubExPhase`, with filter $N = 10$.

The absolute error is small, it equals 4.275833e-10, and the reconstruction after universal thresholding becomes smooth (Figure 4.16).

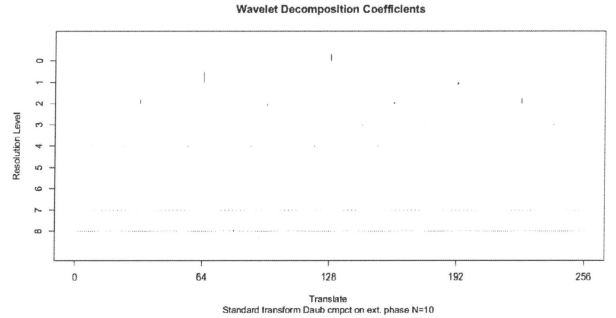

Fig. 4.15. Wavelet coefficients after universal thresholding, `DaubExPhase`, with filter $N = 10$, data on gusts of wind.

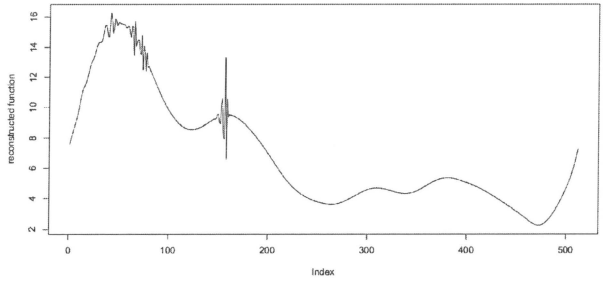

Fig. 4.16. Reconstruction of the data on gusts of wind after universal thresholding, `DaubExPhase`, with filter $N = 10$.

This approach shows that the discrete wavelet transform, based on both – the Haar basis and the Daubechies wavelets, can be an useful tool in investigation of wind potential.

References

[1] Avdakovic S., Lukac A., Nuhanovic A., Music M., Wind Speed Data Analysis using Wavelet Transform, *World Academy of Science, Engineering and Technology*, 75 (2011), 830-834.

[2] Kitagawa T., Nomura T., A wavelet-based method to generate artificial wind fluctuation data, *Journal of Wind Engineering and Industrial Aerodynamics*, 91 (2003), 943-964.

[3] Mielniczuk, Wojdyłło P., Wavelets for time series analysis – a survey and new results, *Control and Cybernetics*, vol. 34 (2005) No. 4., pp.1093-1125.

[4] Nason G., *Wavelet Methods in Statistics with R*, Springer, 2008.

[5] Nason G., Silverman B., The Discrete Wavelet Transform in S, *Journal of Computational and Graphical Statistics*, Vol.3, No. 2 (Jun 1994), pp. 163-191.

[6] Vidakovic, B., Statistical Modeling by Wavelets. Wiley, 1999, New York.